

## Performance Improvements of a Centrifugal Pump with Different Impellers using Polymer Additive

F.Dianatipoor, A. Riasi\*

*School of Mechanical Engineering, College of Engineering, University of Tehran, Tehran, Iran.  
P.O.Box: 11155/4563 Tehran, Iran,*

Received: 4 June. 2017, Accepted: 3 Oct. 2017

### ABSTRACT

*In this study, the performance of a centrifugal pump is investigated by adding polyacrylamide (PAM) polymer over the working fluid which is tap water in this case. PAM is a long chain polymer that leads to reduce the wall shear stress and drag in a turbulent fluid. Three different blade profiles including radial, straight backward and circular backward have been examined. For this purpose, a centrifugal pump test rig consists of reservoir, pump-motor, volumetric measuring tank, pressure gauges, speed control, and motor dynamometer has been used. Different concentrations of PAM polymer solution are prepared in the range of 80-240 ppm of PAM. The results show that the maximum amount of relative efficiency is approximately 3% for the radial propeller, 13% for the straight backward propeller, and 18% for the circular backward which is occurs at 160 ppm of PAM. It is found that this increase is more pronounced in the case of circular backward impeller. Moreover, in the case of radial blade profile, it is observed that in spite of efficiency increase, the head decreases at low flow rate with adding PAM.*

**Keywords:** drag reduction, water pumps, Polyacrylamide polymer, efficiency, blade geometry

---

\* Corresponding Author.

Email Address: [ariasi@ut.ac.ir](mailto:ariasi@ut.ac.ir)

## 1. INTRODUCTION

Nowadays, hydraulic pumps serve in a wide range of application in the industries such as agriculture, refinery, petrochemical, pharmaceutical, etc. The investigation of appropriate solutions to improve the pump performance including efficiency and cavitation is one of the main concerns of the researchers. Ebrahimi et. al. [1] added SiO<sub>2</sub> nanoparticles over the water in a centrifugal pump. The results show that SiO<sub>2</sub> nanoparticles can effectively postpone cavitation initiation and notably decrease the cavitation growth rate. Abuyousef [2] measured a centrifugal slurry pump performance as function of polyacrylamide and pulp fiber concentration. He showed that these additives improve the pump efficiency and there is an optimum concentration for both polyacrylamide and pulp fiber. Ogata [3] added surfactant additives to water and indicated that the performance, maximum flow rate and total head of centrifugal pump are increased with increasing concentration of surfactant.

A small amount of polymer additive such as polyacrylamide (PAM), poly acrylic acid (PAA), polyethylene oxides (PEO) over the water can produce considerable drag reduction especially in the case of turbulent flow. This issue has been the subject of a large number of investigations over the last decades both from theoretical and an experimental point of view. Sellin et al. [4] inferred that non-Newtonian flow effects are not supported by viscometric measurements as an explanation of the drag-reducing effect of polymer solutions. Nowadays, the polymer additives have a growing application in industry, mainly in oil recovery [5], industrial wastewater treatment [6] and pulp and paper industry [7].

The mean velocity profile and friction factor in turbulent flows with drag reduction were studied considering Prandtl's mixing-length model [8]. In the review paper of Benzi [9], the recent ideas for better understanding of drag reduction in an internal turbulent flow has been presented. Based on this study, the polymer chain is stretched by taking energy from the turbulence fluctuations. As a matter of fact, this energy is stored as elastic energy into the polymer chains and then polymer relaxes to the zero stretching during the relaxation time. He showed that the polymer stretching in the perpendicular to the stream wise direction has an important role on drag reduction. This stretching increases linearly as distance from the wall. Later, Housiadas et. al. [10] indicated that it is not just the elasticity but more specifically the exten-

sional deformation that is responsible for the drag reduction. This is manifested primarily at high levels of flow elasticity, which is exhibited at high Weissenberg number, i.e. when the flow time constant is much smaller than the primary time constant (relaxation) of polymeric molecule, but it is also dependent on the nature of the polymer (increase with molecular weight) and its concentration (increase for small concentrations until saturation).

More recently, Zhang et. al.[11] conducted an experimental work on air-water two phase flow heat transfer and pressure drop in a horizontal circular pipe with and without of PAM. This study shows that the pressure drop in the pipe decreases whereas the overall heat transfer decreases as well.

Polymer degradation is a main concern when it is used as drag reducer. As matter of fact, there are three type of degradation consist of: (1) chemical, (2) thermal and (3) mechanical degradation. Mechanical degradation occurs in the pump because of large shear stresses. The polymer should be selected in the way that experiences less degradation. The higher molecular weight is more sensitive to the mechanical degradation [12].

In this study, the performance of centrifugal pumps considering different blade profiles is investigated by adding Polyacrylamide polymer (PAM). Several PAM concentrations are examined in this study. The main objective of the present work is to study the interaction between impeller geometries and polymer additives which is not already investigated. As this purpose three different impellers geometry including radial, straight backward and circular backward have been examined.

## 2. MATERIAL AND METHODS

### 2.1. TEST FLUID

The polyacrylamide (trade name Superfloc A100) is a commercial grade polymer produced by BASF and has molecular weight of 15 Mg/mole as shown in Fig. 1. Polymer concentrations are reported as weight parts per million (ppm) in tap water. The polymer are added to 100 liters of the tap water (Table 1) at concentrations of 80,120,160,200 and 240 ppm. The solution was slowly agitated (at low speed) for one hour in the tank to insure the homogeneity of the mixture. Each concentration test was performed separately to avoid degradation and the temperature of fluids in all tests (including the tap water test) is about 18 – 22°C. Rheologically, these test solutions behave as Newtonian fluids because their concentrations are less than 400 ppm [4, 13].

Table 1. Tap water quality parameters

PH	TDS (ppm)	Cl (ppm)	SO4 (ppm)	Mg (ppm)	K (ppm)	Na (ppm)
7.89	690	151.26	103.38	25.74	3.46	95.73

Moreover, the viscosity variation at the maximum concentration in this study (240 ppm) is less than 3 cSt [13]. Regarding the available viscosity correction chart, all of the performance correction coefficients for this range of viscosity are almost one. This fact shows that the viscosity does not effect on the pump performance for this range of concentrations

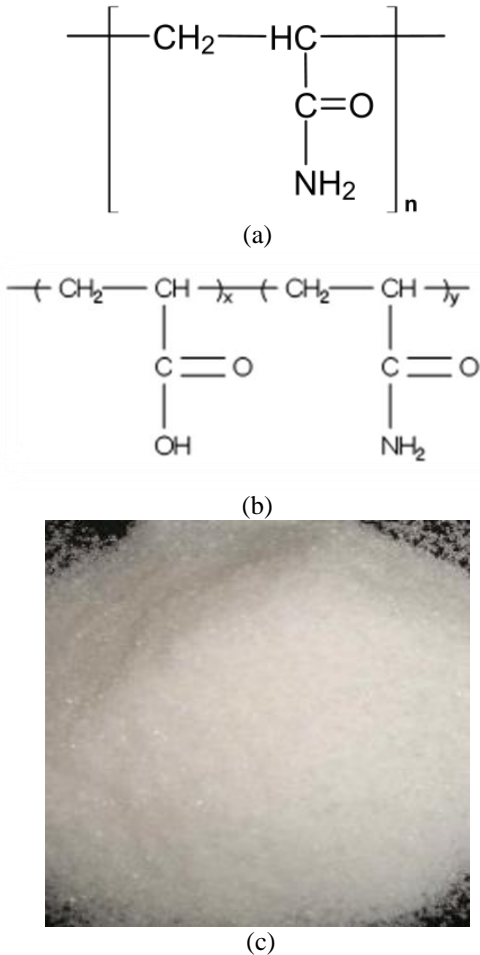


Fig. 1. (a) Chemical structure of PAM  $(C_3H_5NO)_n$ , (b) Neutral form of Superfloc A100 and (c) Superfloc A100 particles

2.2. TEST RIG

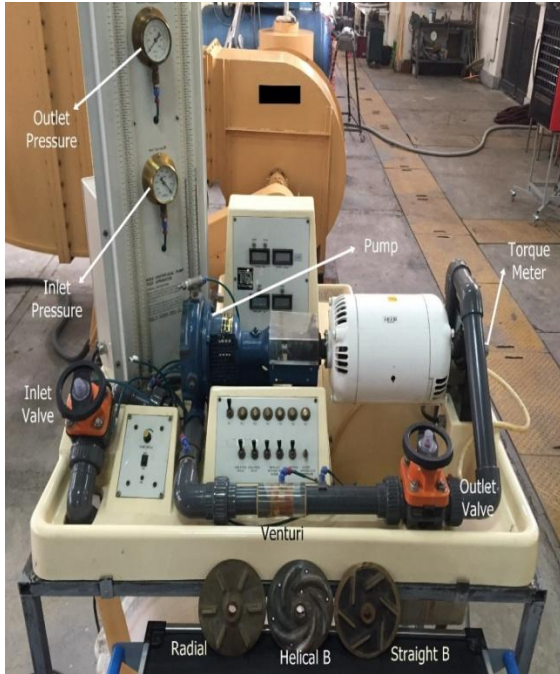
The centrifugal pump test rig is situated on a hydraulic bench and consists of reservoir, pump-motor, volumetric measuring tank, pressure gauges, speed control, motor dynamometer, etc. In addition, the main control equipment is located in easily-accessible places. The speed-regulation valve is located in left side of the table, a pressure control panel in the middle, a digital display panel in the rear side, the inlet suction valve in the left side, the outlet pressure valve (flow rate regulator) and the dynamometer (for measuring torque) are in the right side of the table. Manometers and pressure gauges are set in the left side of the table to be used easily in working conditions (Fig. 2a).

Fig. 2b depicts a schematic view of this apparatus. The water flow direction is shown in this figure. Water is conducted to the pump via a foot valve and then a diaphragm valve. Through the discharge pipeline which crosses the front part of the table, water runs forward to a flow rate-regulation valve and then into a volumetric measuring tank for flow metering. Finally, water returns to the main reservoir of the system through an overflow system or the valve on the bottom of the volume-meter reservoir. It is worth mentioning that several pressure taps are installed before and after the pump for pressure measuring.

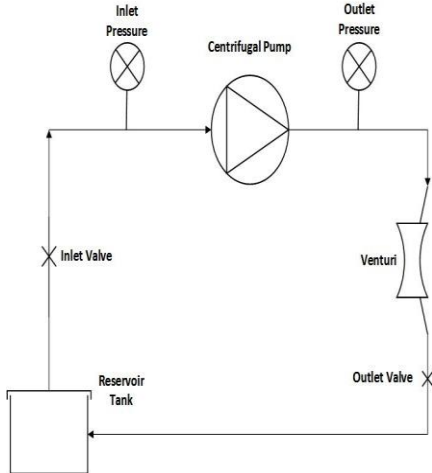
Fig. 3 shows three impellers with different blade profiles have been examined in this study including (a) straight backward blade profile, (b) circular backward blade profile and (c) radial blade profile. All three impellers have the same diameter. The details characteristics of these impellers are listed in Table 2.

Table 2. Geometric characteristics of blades

Impeller	Diameter (mm)	Number of Blades	Inlet Blade Angle ( $\beta_1$ )	Outlet Blade Angle ( $\beta_2$ )
Radial	165	6	90	90
Straight Backward	165	6	15	60
Circular Backward	165	6	15	22.5



(a)



(b)

Fig. 2. (a) Test rig and examined impellers, (b) schematic view of test rig

$$H_p = \left( \frac{P}{\rho g} + \frac{V^2}{2g} + Z \right)_{Inlet} - \left( \frac{P}{\rho g} + \frac{V^2}{2g} + Z \right)_{Outlet} \quad (1)$$

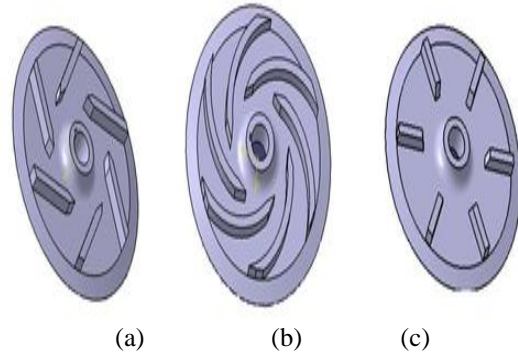
$$\eta_p = \frac{\rho g H_p Q}{\tau \omega} \quad (2)$$

In which  $H_p$  and  $\eta_p$  are the pump head and efficiency, respectively.  $P$  is static pressure,  $V$  is velocity,  $Z$  stands for elevation,  $Q$  is the pump flow rate,  $\tau$  is the shaft torque,  $\rho$  is the fluid density and  $\omega$  presents the rotational speed. In the next step the pump characteristics are plotted.

### 2.3. TEST PROCEDURE

The experimental procedure consists of two steps:

1. All three types of impeller including radial, straight backward, and circular backward are tested using tap water as working fluid. As this purpose the discharge valve is varied from fully open to closed position and at each state of valve opening the following variables are measured: (1) pump inlet pressure, (2) pump outlet pressure, (3) pump flow rate, (4) pump rotational speed and (5) shaft torque. Regarding the measured data head and efficiency of pump are calculated as:



(a)

(b)

(c)

Fig. 3. Different impellers used in this study, (a) Straight backward blade profile, (b) Circular backward blade profile and (c) Radial blade profile

2. Polymer additive is added to the water to make desirable concentrations of solution and all three type of impeller are examined. Then, according to the measured data the characteristics curves are plotted. The test conditions are listed in Table 3.

Table 3. Test conditions

	1 <sup>st</sup> Part	2 <sup>nd</sup> Part
<b>Pump Rotational Speed</b>	1750 rpm	1750 rpm
<b>Working Fluid Properties</b>	Tap water 18°C/ 21°C	Tap water + PAM, 18°C/ 21°C

### 3. UNCERTAINTY ANALYSIS

To assess the accuracy of the measurement, the uncertainty analysis should be performed. Considering the experimental results which are determined from  $j$  measured variables as:

$$w_r = \left[ \left( \frac{\partial r}{\partial X_1} w_1 \right)^2 + \left( \frac{\partial r}{\partial X_2} w_2 \right)^2 + \dots + \left( \frac{\partial r}{\partial X_j} w_j \right)^2 \right]^{1/2} \quad (4)$$

where  $w_j$  is the uncertainty of the measurements. From this equation the average uncertainty for head coefficient and efficiency is less than 0.15% and 2%, respectively in this study.

### 4. RESULT AND DISCUSSION

Firstly, the non-dimensional head and flow coefficients are defined as:

$$\Psi = \frac{gHP}{\omega^2 D^2} \quad (5)$$

$$\Phi = \frac{Q}{\omega D^3} \quad (6)$$

where  $\Psi$  and  $\Phi$  are the head and flow coefficients, respectively and  $D$  presents impeller diameter.

The diagram of Head coefficient ( $\Psi$ ) versus flow coefficient ( $\Phi$ ) for various types of pump impellers is shown in Fig. 4. As shown in this figure, the curve of the tap water has been compared with solutions whose PAM concentrations are 80,120,160,200,240 ppm. Similarly, the diagram of efficiency versus flow coefficient is shown in Fig. 5.

It is clear from these figures, head and efficiency increases even in the cases of small concentration of PAM and this increase is more pronounced for circular backward blade profile. This can be interpreted considering the greater blade length of circular backward type in comparison with two other types. In this condition the flow passage is long and as consequence the wall friction is more. Therefore, the drag reduction is larger because of the viscoelastic effect of PAM solution. As it is earlier described, the turbulence energy is stored via stretching the polymer chains and as consequent the turbulence dissipation decreases. It is a well mentioning that the flow rate is approximately equal for the all impellers. Another hypothetical consideration is that because of the flow pattern in the flow passage of the radial blade profile, the shear stresses increase and results in more polymer degradation [18]. Therefore, the rate of drag reduction decreases.

$$r = r(X_1, X_2, \dots, X_j) \quad (3)$$

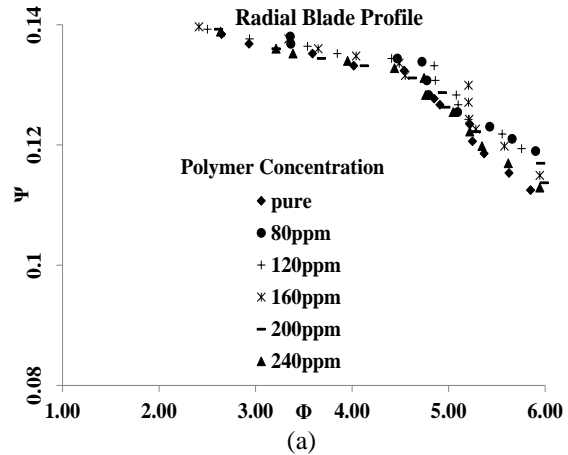
The uncertainty of the result,  $w_r$ , is found as [14]:

To have a deep insight about the effect of PAM additives, a comparison between tap water and PAM solution are made through the following relative Parameters:

$$\eta^* = \frac{\eta_{PAM} - \eta_{Water}}{\eta_{Water}} \times 100 \quad (7)$$

$$\Psi^* = \frac{\Psi_{PAM} - \Psi_{Water}}{\Psi_{Water}} \times 100 \quad (8)$$

In which  $\eta_{PAM}$  and  $\eta_{Water}$  state the efficiency for PAM solution and tap water and also  $\Psi_{PAM}$  and  $\Psi_{Water}$  present the head coefficient for PAM solution and tap water. Fig. 6 depicts the diagrams of  $\eta^*$  and  $\Psi^*$  versus ppm of PAM solution. Fig. 6(a) and 6(b) are plotted for the best efficiency point at each ppm of PAM. Regarding this figure,  $\eta^*$  and  $\Psi^*$  achieve their maximum peak values at 160 ppm. In the case of circular backward blade profile, the head and efficiency improvement is considerable.



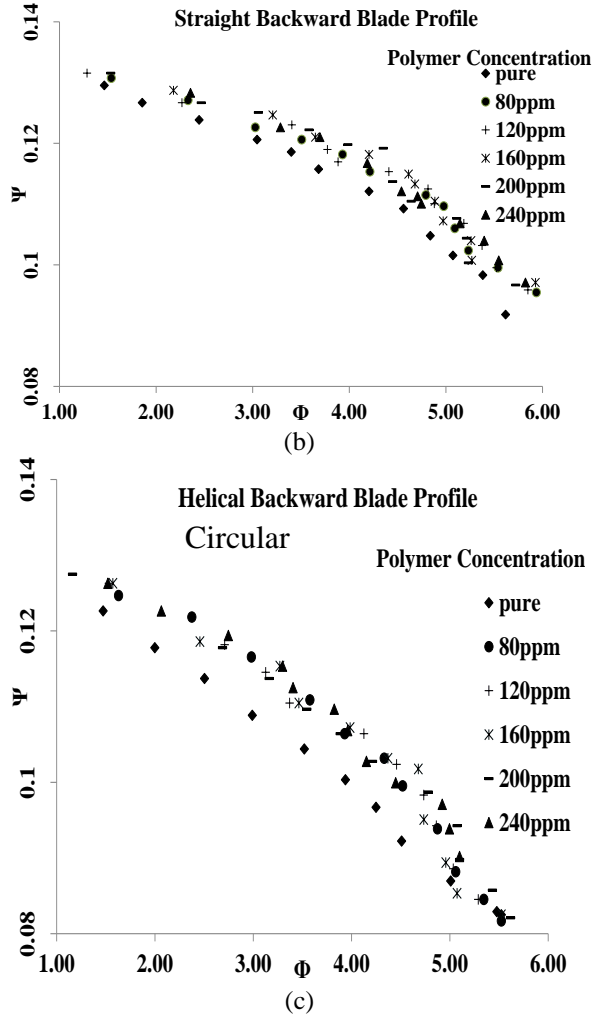


Fig. 4  $\Psi$ - $\Phi$  diagram for (a) Radial blade profile, (b) Straight backward blade profile and (c) Circular backward blade profile

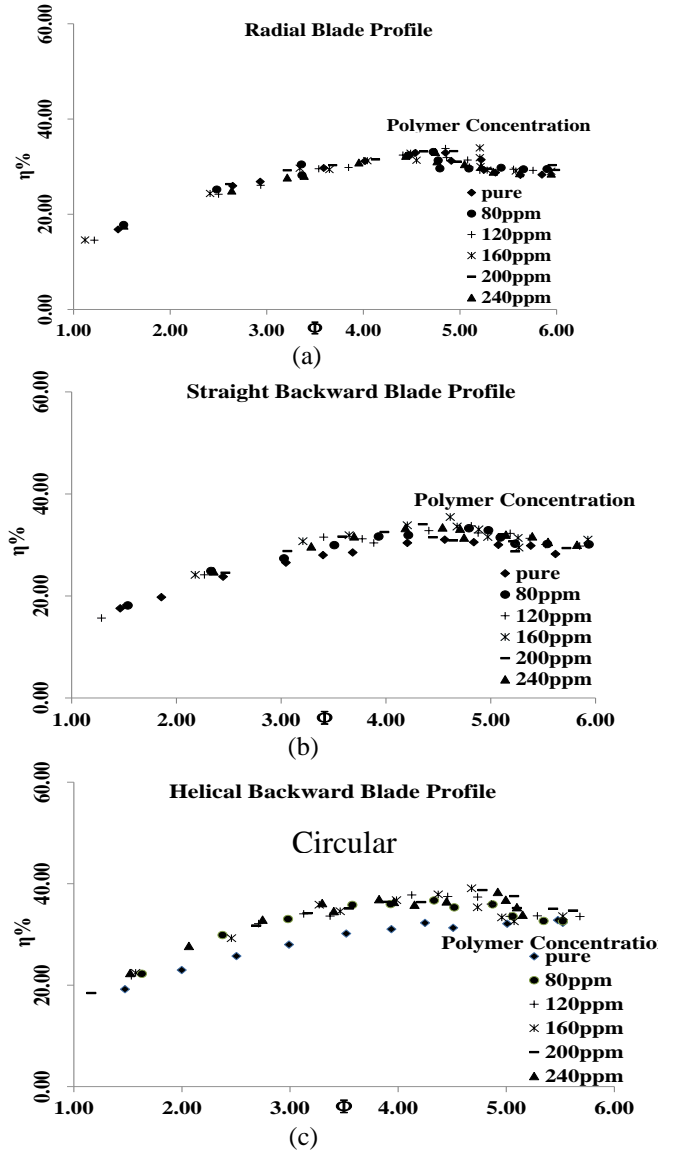


Fig. 5  $\eta$ - $\Phi$  diagram for (a) Radial blade profile, (b) Straight backward blade profile and (c) Circular backward blade profile

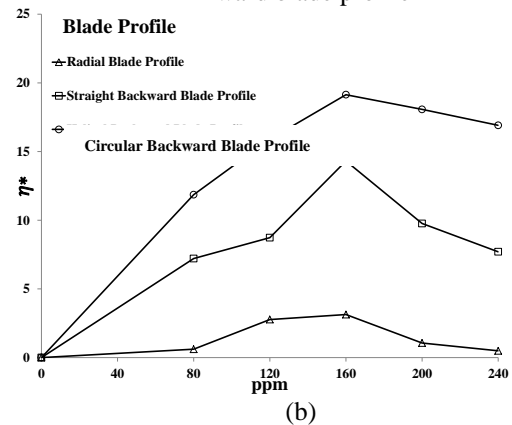
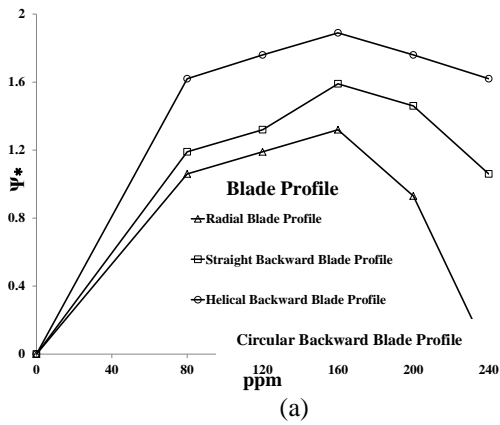


Fig. 6 (a) Diagram of  $\Psi^*$  versus ppm of PAM at best efficiency point, (b) Diagram of  $\eta^*$  versus ppm of PAM at the best efficiency point

Fig. 7 shows the diagram of  $\eta^*$  and  $\Psi^*$  versus ppm of PAM solution for three type of impeller at the off-design point in which the flow coefficient set to be 2. Regarding this figure, the best ppm concentration is different for each impeller. As shown in Fig. 7(a), the amount of  $\Psi^*$  for circular and straight backward blade is greater in comparison with those obtained for  $\Psi^*$  at the best efficiency point (Fig. 6a). The main reason for this issue is that the hydraulic losses in the pump due to separation and vortex flows are considerably increased at the off-design point and as consequent turbulence intensity increases and it is expected that the PAM additive as drag reducer to be more affective. In the case of radial blade profile, the amount of  $\Psi^*$  is negative whereas  $\eta^*$  is positive. This finding can be interpreted considering Eq. 2. In

this case the percent decrease of torque is greater than the percent decrease of head for the different ppm of PAM solutions. Therefore, in spite of efficiency increase, the head decreases. The main reason for the head decrease in the radial blade profile is maybe due to the jet and wake pattern through the impeller passage. Jet and wake occurs because of the boundary layer separation on the suction side of blade, especially at the low flow rate. In the case of the radial blade the separation point is close to the blade leading edge and as a result the dead region at the blade outlet is greater. This dead region changes the blade outlet angle and results in slip factor and head reduction. So, PAM changes the flow pattern through the blade passage and changes the jet and wake pattern and seems this effect dominates over the drag reduction effect of polymer.

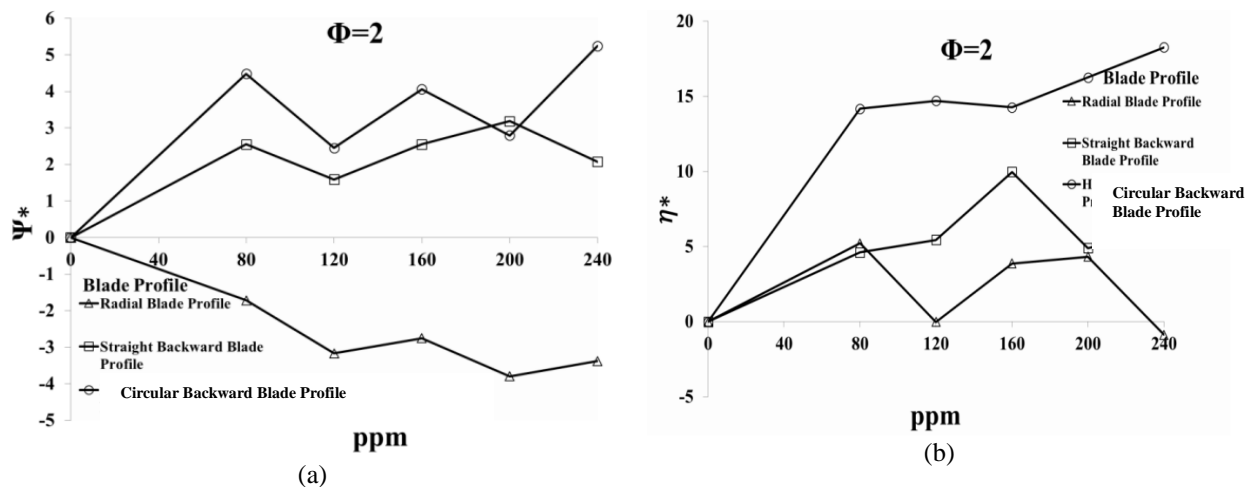


Fig. 7 (a) Diagram of  $\Psi^*$  versus ppm of PAM at  $\Phi=2.0$  (b) Diagram of  $\eta^*$  versus ppm of PAM at  $\Phi=2.0$

## CONCLUSION

This study shows that even small amounts of PAM polymer may improve the pump performance including the head and efficiency. The best concentration for all three type of blade is 160 ppm. The amount of maximum relative efficiency ( $\eta^*$ ) is approximately 3% for the radial propeller, 13% for the straight backward propeller, and 18% for the circular backward. In the case of the off-design point, the percent increase of the head is greater than the case of best efficiency point, due to the more hydraulic losses occurs at the off-design point. Moreover, it is observed that PAM changes the flow outlet angle in the case of radial blade and as a result the pump head decrease at the off-design point. Future studies should focus on detecting the onset of cavitation phenomena in presence of polymer additives.

## REFERENCES

- [1] Bidhandi, M. E., Riasi, A., & Ashjaee, M. (2014). The influence of SiO<sub>2</sub> nanoparticles on cavitation initiation and intensity in a centrifugal water pump. *Experimental Thermal and Fluid Science*, 55, 71-76.
- [2] AbuYousef, I. A., Olson, J. A., Martinez, D. M., & Green, S. (2010, January). Pumping Performance Increase through the Addition of Turbulent Drag-Reducing Polymers to Pulp Fibre Suspensions. In *ASME 2010 International Mechanical Engineering Congress and Exposition* (pp. 709-718). American Society of Mechanical Engineers.
- [3] Ogata, S., Kimura, A., & Watanabe, K. (2006). Effect of surfactant additives on centrifugal pump performance. *Journal of Fluids Engineering*, 128(4), 794-798.
- [4] Sellin, R. H. J., Hoyt, J. W., & Scrivener, O. (1982). The effect of drag-reducing additives on fluid flows and their industrial applications part 1: basic aspects. *Journal of Hydraulic Research*, 20(1), 29-68.

- [5] Thomas, A., Gaillard, N., & Favero, C. (2012). Some key features to consider when studying acrylamide-based polymers for chemical enhanced oil recovery. *Oil & Gas Science and Technology—Revue d'IFP Energies nouvelles*, 67(6), 887-902.
- [6] Barvenik, F. W. (1994). Polyacrylamide characteristics related to soil applications. *Soil Science*, 158(4), 235-243.
- [7] Smook, G. A. (2002). *Handbook for pulp & and paper technologists*. Angus Wilde Publ., 218-221.
- [8] Yang, S. Q. (2009). Drag reduction in turbulent flow with polymer additives. *Journal of Fluids Engineering*, 131(5), 051301.
- [9] Benzi, R. (2010). A short review on drag reduction by polymers in wall bounded turbulence. *Physica D: Nonlinear Phenomena*, 239(14), 1338-1345.
- [10] Housiadas, K. D., & Beris, A. N. (2013). On the skin friction coefficient in viscoelastic wall-bounded flows. *International Journal of Heat and Fluid Flow*, 42, 49-67.
- [11] Zhang, X., Liu, L., Cheng, L., Guo, Q., & Zhang, N. (2013). Experimental study on heat transfer and pressure drop characteristics of air–water two-phase flow with the effect of polyacrylamide additive in a horizontal circular tube. *International Journal of Heat and Mass Transfer*, 58(1), 427-440.
- [12] Thomas, A., Gaillard, N., & Favero, C. (2012). Some key features to consider when studying acrylamide-based polymers for chemical enhanced oil recovery. *Oil & Gas Science and Technology—Revue d'IFP Energies nouvelles*, 67(6), 887-902.
- [13] Bjorneberg, D. L. (1998). Temperature, concentration, and pumping effects on PAM viscosity. *Transactions of the ASAE*, 41(6), 1651-1655.
- [14] ASME V&V 20, Standard for Verification and Validation in Computational Fluid Dynamics and Heat Transfer, 2009.